

# PERMEABILITY, POROSITY AND KLINKENBERG COEFFICIENT DETERMINATION ON CRUSHED POROUS MEDIA

Sandra Profice<sup>1</sup>, Didier Lasseux<sup>1</sup>, Yves Jannot<sup>2</sup>, Naime Jebara<sup>3</sup> and Gérald Hamon<sup>3</sup>

<sup>1</sup> I2M-TREFLE, Université de Bordeaux, CNRS

Esplanade des Arts et Métiers - 33405 Talence

<sup>2</sup> LEMTA, Nancy-Université, CNRS

2, avenue de la Forêt de Haye, BP 160 - 54504 VANDOEUVRE Cedex - France

<sup>3</sup> TOTAL – CSTJF – Avenue Larribau – 64018 Pau Cedex – France

*This paper was prepared for presentation at the International Symposium of the Society of Core Analysts held in Austin, Texas, USA 18-21 September, 2011*

## ABSTRACT

Permeability estimation of poor permeable formations like tight or gas shale reservoirs using a pulse decay experiment performed on crushed samples has been shown in earlier works to be an interesting alternative for it is cheaper and faster than traditional transient tests performed on carefully prepared core plugs; although it is restricted to measurement in the absence of overburden pressure. Due to reservoir depletion during production, sample characterization over a wide range of pore fluid pressure is essential. If the Darcy-Klinkenberg model is thought to be a satisfactory gas flow model for these tight formations, the full characterization can be achieved by determining both the intrinsic permeability,  $k_i$ , and Klinkenberg coefficient,  $b$ .

In this work, the conditions under which reliable estimates of  $k_i$ ,  $b$  and porosity,  $\phi$  can be expected from this type of measurement are carefully analyzed. Considering a bed of monodisperse packed spheres and a complete physical model to carry out direct simulations and inversion of the pressure decay, important conclusions are drawn opening wide perspectives for significant operational improvement of the method. In particular, it is shown that:

- i)* The particle size of the crushed sample must be well selected for a reliable pressure decay signal record.
- ii)* The simultaneous determination of both  $k_i$ , and  $b$  by inversion of the pressure decay signal is made very difficult because the sensibilities of the pressure decay to both coefficients are correlated.
- iii)* The porosity of the particles can be accurately estimated when the experimental setup has been well calibrated (volumes of the chambers and of the porous sample). The precision on the estimation of this parameter is however strongly dependent on a bias on the crushed sample volume.
- iv)* When the identification of the  $k_i$ , and  $b$  is possible, a very significant error may occur on the intrinsic permeability due to a bias on the porous sample volume. Errors on the estimated values of  $\phi$  and  $k_i$  due to a bias on the chamber volume are not very significant. Moreover,  $b$  remains insensitive to bias on both the chamber and porous sample volumes.

## INTRODUCTION

Due to the great amount of natural gas they are likely to provide, gas shales have become a topic of major interest over the past 10 years. Their reliable characterization is however a challenging task since these unconventional reservoirs have very tight pores and therefore specific flow properties, in particular very significant Klinkenberg effects at least after a sufficiently long period of reservoir depletion. These special features call upon a careful identification of tractable and reliable methods to determine one-phase flow properties that are of major importance to evaluate accumulation and production capabilities of the reservoir. Since depletion of the reservoir may take place over a wide range of pore pressure, and provided one admits that the Darcy-Klinkenberg model is a valid one to account for one-phase gas flow in such a porous medium, a characterization of porosity  $\phi$ , intrinsic permeability  $k_i$ , and Klinkenberg coefficient  $b$ , should give relevant insights in the reservoir properties.

Since the permeability of shales ranges from tens of microdarcies to nanodarcies, time to reach stationary flow while performing a steady-state experiment on such samples is relatively long (it typically varies as the inverse of  $k_i$ ) even on short plugs. Whereas associated flow rates are small (and difficult to measure), it must be noted that the separate determination of  $k_i$  and  $b$  requires several different experiments when performed under steady-state conditions. Although this technique is widely used, alternative methods based on unsteady techniques are hence appealing. In the late 60's, Brace *et al.* [1] elaborated the pulse decay technique which consists in applying a pressure pulse at one end of a core plug while recording the response at the opposite end. Since then, countless works aimed at improving the setup and associated interpretation of the results. More recently, Luffel *et al.* [2] proposed to carry out a pulse decay on a crushed sample. It consists in recording the unsteady step of a pycnometry-type experiment using a device schematically represented in Fig. 1.

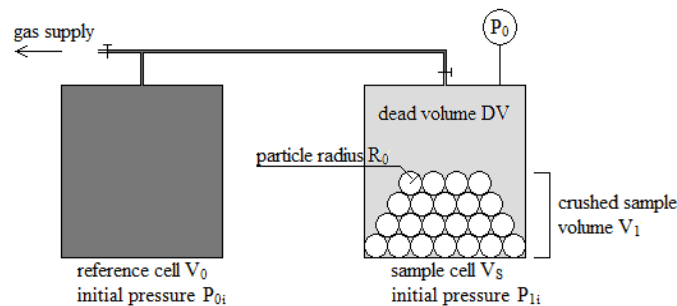


Figure 1. Schematic experimental setup

This option is particularly appealing as it obviously shortens the test duration, by increasing the medium exchange area with the penetrating gas while decreasing the penetration depth. In addition, the test cost is reduced since only few cuttings recovered during the drilling are enough for the analysis. However, experiments under realistic overburden pressures are impossible.

Several variations of this technique were envisaged. For instance, Egermann *et al.* [3] proposed a technique based on flow of a viscous oil within saturated cuttings leading to a compression of the residual gas content. Other procedures can be quoted like those

proposed by Luffel et al. [2] and later by Lenormand et al. [4] who introduced similar methods relying on the gas desorption of entire plugs subjected to a suction or vacuum. Recently, Wang and Knabe [5] worked on a pore pressure oscillation setup based on the generation of a sinusoidal excitation at the upstream side of a sample that is pre-conditioned at a given pore pressure.

All these transient tests are highly sensitive to the medium porosity which governs the transient gas flow. If this parameter is considered as a given datum in the interpretative model, it must be known with extreme accuracy, estimates of the remaining parameters being severely biased otherwise. As a consequence, a method allowing the determination of all the three parameters ( $k_1$ ,  $b$  and  $\phi$ ) from a single experiment is highly desirable.

The purpose of the present work is to analyze the capabilities of a pulsed decay experiment performed on a crushed sample to fulfill this request. To do so, a physical model describing a model configuration is implemented and validated by an approximated analytical solution. Both the direct and inverse procedures are derived allowing to *i*) investigate the available information in the pressure decay record that is strongly related to the radius of the particles of the crushed sample; *ii*) analyze the possibility of extracting the three parameters  $k_1$ ,  $b$  and  $\phi$  from the pressure decay signal using a sensitivity analysis and *iii*) study the impact of the chamber and sample volume bias on the estimated parameters when inversion is possible.

## PROCEDURE

### Modeling

The pulse decay experiment carried out on the crushed sample must be first described by the flow model.

#### Direct Model

The physical model built to describe the pulse decay experiment on a crushed sample relies on several hypothesis. First of all, the gas is supposed to be ideal, a commonly used approximation that is well-suited for gases like  $N_2$  or He at operating pore pressures. Furthermore, the flow is assumed to be isothermal and slow enough to prevent development of inertial (Forchheimer) effects. At the pore level, a first order slip flow is considered, yielding a Darcy-Klinkenberg flow model at the macro-scale. Lastly, the crushed medium is assimilated to a monodisperse sphere pack, the porous material being rigid, homogeneous isotropic and dry while pressure is assumed to be uniform in the spaces between spherical particles at any time. Under these circumstances, the flow is one-dimensional along the radial direction of each sphere and is described by the following equation on the pressure  $P$  at the position  $r$  in each particle at time  $t$  by combining the mass-conservation equation with the ideal gas law and the momentum conservation equation (Darcy-Klinkenberg), yielding

$$\frac{\phi \mu \partial P}{k_1 \partial t} = \frac{1}{r^2} \frac{\partial}{\partial r} \left( r^2 (P + b) \frac{\partial P}{\partial r} \right) \quad (1)$$

The associated initial and boundary conditions are given by:

$$P_0(t = 0) = P_{0i} \quad (2)$$

$$P(r \neq R_0, t = 0) = P_{1i} \quad (3)$$

$$\left(\frac{\partial P}{\partial r}\right)_{r=0} = 0 \quad (4)$$

$$-\frac{\mu(V_0 + DV)}{S_T k_l} \left(\frac{\partial P}{\partial t}\right)_{r=R_0} = (P_0 + b) \left(\frac{\partial P}{\partial r}\right)_{r=R_0} \quad (5)$$

Equation (3) indicates that the system is initially at equilibrium with the surrounding atmosphere at  $P_{1i}$  prior to the emission of the pressure pulse at  $t=0$  (Eq. (2)). The condition (4) simply results from the symmetry of the problem while Eq. (5) expresses the balance between the mass flow-rate coming in all the particles of total surface area  $S_T$  and the mass flow rate out of the volume of gas available to the particles,  $V_0+DV$ . The interest is focused on  $P_0(t)=P(r=R_0,t)$  which is the pressure in the reservoir  $V_0+DV$  as measured in the experiment.

This initial boundary value problem has no analytical solution. It was hence solved by means of a numerical procedure, specifically an explicit difference scheme of first order in time and second order in space, inspired from previous works on the pulse decay experiment on core plugs [6].

#### Approximated Analytical Solution

The numerical scheme was validated on a simplified configuration where an analytical solution can be determined. For this analytical solution to be tractable, some simplifications are required. The first one consists in neglecting the Klinkenberg effect so that Eqs. (1) to (5) can be re-written as:

$$\frac{\phi \mu k_l}{k_l P} \frac{\partial \psi}{\partial t} = \frac{1}{r^2} \frac{\partial}{\partial r} \left( r^2 \frac{\partial \psi}{\partial r} \right) \quad (6)$$

$$\psi(r = R_0, t = 0) = P_{0i}^2 \quad (7)$$

$$\psi(r \neq R_0, t = 0) = P_{1i}^2 \quad (8)$$

$$\left(\frac{\partial \psi}{\partial r}\right)_{r=0} = 0 \quad (9)$$

$$-\frac{\mu(V_0 + DV)}{S_T k_l} \frac{1}{P} \left(\frac{\partial \psi}{\partial t}\right)_{r=R_0} = \left(\frac{\partial \psi}{\partial r}\right)_{r=R_0} \quad (10)$$

with:

$$\psi = P^2 \quad (11)$$

Because of the persisting non-linearity due to the term  $1/P$  in equations (6) and (10), this new problem has still no analytical solution. For a perfect gas,  $1/P$  represents the fluid compressibility  $\beta_f$ . To circumvent the difficulty, it is further assumed that  $\beta_f$  is constant, which should be reasonable if the pressure experiences only slight fluctuation during the test. Under these circumstances, the problem can be solved analytically.

The sequence of derivation of the solution splits in two parts. The set of equations is first Laplace transformed and solved in the Laplace domain. The solution is inverted making use of the Cauchy theorem, as detailed by Hsieh *et al.* [7] in a second step. Following this procedure, the analytical solution on  $P_0(t)$  is obtained as:

$$P_0(t) = \sqrt{\frac{3\gamma K}{3\delta K R_0^2 + R_0^3} + \frac{2}{R_0} \sum_m \frac{\gamma K \exp\left(\frac{-\xi_m^2 K}{R_0^2} t\right) \sin(\xi_m)}{R_0 [\delta K \xi_m \cos(\xi_m) + (R_0 + 2\delta K) \sin(\xi_m)]} + P_{11}^2} \quad (12)$$

with:

$$\gamma = \delta R_0^2 (P_{01}^2 - P_{11}^2) \quad (13)$$

$$\delta = \frac{\mu(V_0 + DV)\beta_f}{S_f k_l} \quad (14)$$

and:

$$K = \frac{k_l}{\phi \mu \beta_f} \quad (15)$$

The  $\xi_m$  are the roots of:

$$\tan(\xi_m) = \frac{\xi_m}{1 + \frac{\delta K \xi_m^2}{R_0}} \quad (16)$$

On Fig. 2, we have represented the evolution of  $P_0$  obtained from the numerical method along with the evolution predicted by the analytical solution given by Eq. (12). Parameters used for this comparison are  $k_l=10^{-18}$  m<sup>2</sup>,  $b=0$  Pa,  $\phi=10$  %,  $R_0=10^{-2}$  m,  $V_0=20 \cdot 10^{-6}$  m<sup>3</sup>,  $V_1=75.4 \cdot 10^{-6}$  m<sup>3</sup>,  $DV=26.5 \cdot 10^{-6}$  m<sup>3</sup>,  $P_{01}=10 \cdot 10^5$  Pa,  $P_{11}=10^5$  Pa,  $\mu=1.8 \cdot 10^{-5}$  Pa.s,  $t_f=60$  s,  $NP=1200$ ,  $m=500$  (see nomenclature for the significance of the different parameters).

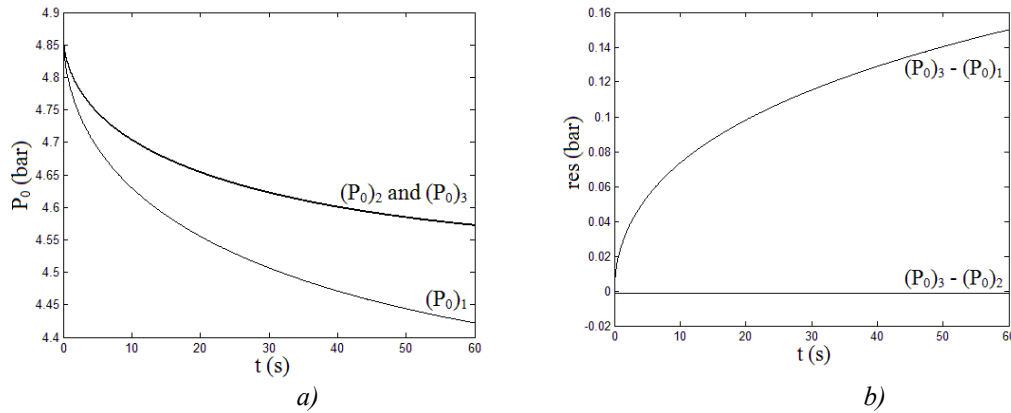


Figure 2. a) Numerical and analytical pressure decay curves.  $(P_0)_1$ : numerical pressure decay keeping a variable  $\beta_f$ ;  $(P_0)_2$ : numerical pressure decay for a constant  $\beta_f$ ;  $(P_0)_3$ : analytical pressure decay for a constant  $\beta_f$ . b) Residues drawn from the comparison of  $(P_0)_1$  and  $(P_0)_2$  to  $(P_0)_3$

The crushed sample volume  $V_1$  was fixed to that of the standard core plug and the space trapped between the spheres, i.e. the dead volume  $DV$ , was calculated assuming that the spherical particles are packed according to a perfect face-centered cubic lattice which compactness reaches 74 %. Note that for real crushed samples for which particle shapes may strongly deviate from sphericity, larger compactness, i.e. smaller  $DV$ , may be achieved.

In order to estimate the deviation introduced by the hypothesis of a constant compressibility, the numerical procedure was first run keeping a variable  $\beta_f$  (i.e. keeping  $P$  as an evolving variable in the term  $1/P$  in equations (6) and (10)) yielding  $P_0(t)$  represented

as  $(P_0)_1$  in Fig. 2a. In a second step, the numerical procedure was run using the same parameters with a constant  $\beta_f$  equal to  $1/P_m$ ,  $P_m$  being the time average over  $t_f$  of  $(P_0)_1$ . The corresponding result is represented as  $(P_0)_2$  in Fig. 2a. The analytical solution in this last situation is represented as  $(P_0)_3$  in Fig. 2a.

The numerical and analytical results for a constant  $\beta_f$  are in perfect agreement since the residue (see figure 2b) remains globally close to 1mbar for the chosen number of space nodes. The matching can even be improved when  $m$  is increased. This comparison clearly validates our numerical procedure. The comparison between the analytical solution and the numerical one simulated with a variable  $\beta_f$  shows a much more significant discrepancy that increases with time as suggested in [8]. Hence, even if the pressure decay remains small during the test, the constant gas compressibility assumption may introduce a significant error and should not be considered as a valid one for further parameter identification since uncontrolled bias may be introduced. The numerical procedure is now used to analyze the impact of the different experimental parameters on the pulse decay test.

## RESULTS AND DISCUSSION

In this section, the numerical procedure is used to investigate the impact of the particle size of the crushed sample on the pressure decay and to perform a sensitivity analysis of  $P_0(t)$  to the parameters  $k_i$ ,  $b$  and  $\phi$ . An inverse procedure based on the direct numerical model is further employed to analyze the bias on  $V_0$  and  $V_1$  on the estimated values of  $k_i$ ,  $b$  and  $\phi$  when the estimation is possible.

### Duration of the Experiment

Several numerical tests performed with a particle size  $R_0$  of the crushed sample ranging from 1mm to 1cm were performed keeping all other parameters the same, namely,  $k_i=10^{-21}$  m<sup>2</sup>,  $b=68.6 \cdot 10^5$  Pa,  $\phi=1$  %,  $V_0=20 \cdot 10^{-6}$  m<sup>3</sup>,  $V_1=75.4 \cdot 10^{-6}$  m<sup>3</sup>,  $DV=26.5 \cdot 10^{-6}$  m<sup>3</sup>,  $P_{0i}=50 \cdot 10^5$  Pa,  $P_{1i}=10^5$  Pa,  $\mu=1.8 \cdot 10^{-5}$  Pa.s,  $t_f=200$  s,  $NP=2000$  and  $m=200$ . Results of the simulations are reported in Fig. 3.

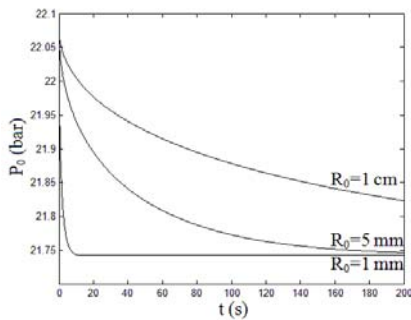


Figure 3. Pressure decay curves for different  $R_0$

From these results, it must be emphasized that the period over which the pressure decays and holds useful information about the physical parameters  $k_i$ ,  $b$  and  $\phi$  is strongly related to the grain size. In fact, this characteristic dimension determines the test duration as it is approximately divided by 10 when the particle radius is decreased from 1cm to 1mm. Thus, the smaller the spheres, the faster the decay, an acceleration that can be easily understood as the result of an increase of the exchange surface  $S_T$  in conjunction with a reduction of the characteristic dimension to be

penetrated by the pressure signal while reducing  $R_0$ ,  $V_1$  remaining the same. However, just a few seconds of recording (as for  $R_0=1\text{mm}$ , see Fig. 3) are insufficient to guarantee an accurate post-estimation of the medium properties, taking into account actual pressure fluctuations at short times induced by valve opening and induced temperature effects resulting from the rapid gas expansion from  $V_0$  to  $V_0+DV$  which are not considered in this model. Consequently, for a given rock and predefined experimental conditions, the mean grain size must be carefully selected to provide a usable signal for the estimation of  $k_1$ ,  $b$  and  $\phi$  by signal inversion. This dimension must even be considered as more crucial while considering real particle shapes. Indeed, the hypothesis of spherical particles implies that the surface-to-volume ratio is minimum. Hence the time to reach final pressure equilibrium is maximum and with particles of arbitrary shape having the same average dimension, the available pressure decay signal is expected to be even shorter.

### Sensitivity Analysis

We now analyze the sensitivity of  $P_0(t)$  to the parameters that are to be estimated, namely  $k_1$ ,  $b$  and  $\phi$ . Several runs were performed with  $\phi = 10\%$ ,  $R_0=10^{-2}\text{ m}$ ,  $V_0=20 \cdot 10^{-6}\text{ m}^3$ ,  $V_1=75.4 \cdot 10^{-6}\text{ m}^3$ ,  $DV=26.5 \cdot 10^{-6}\text{ m}^3$ ,  $P_{0i}=50 \cdot 10^5\text{ Pa}$ ,  $P_{1i}=10^5\text{ Pa}$ ,  $\mu=1.8 \cdot 10^{-5}\text{ Pa}\cdot\text{s}$ ,  $t_f=12600\text{ s}$ ,  $NP=12600$  and  $m=200$ . The remaining parameters  $k_1$  and  $b$  were those reported in table 1. Numerical results obtained on  $P_0(t)$  for the different  $(k_1, b)$  pairs are represented in figure 4.

Table 1.  $(k_1, b)$  pairs used for the simulations of figure 4

$k_1\text{ (m}^2\text{)}$	$b\text{ (Pa)}$
$2.26 \cdot 10^{-21}$	$22.4 \cdot 10^5$
$2.12 \cdot 10^{-21}$	$24.8 \cdot 10^5$
$1.56 \cdot 10^{-21}$	$38.9 \cdot 10^5$
$1.00 \cdot 10^{-21}$	$68.6 \cdot 10^5$
$7.89 \cdot 10^{-22}$	$90.7 \cdot 10^5$
$6.21 \cdot 10^{-22}$	$11.9 \cdot 10^6$
$2.84 \cdot 10^{-22}$	$27.8 \cdot 10^6$

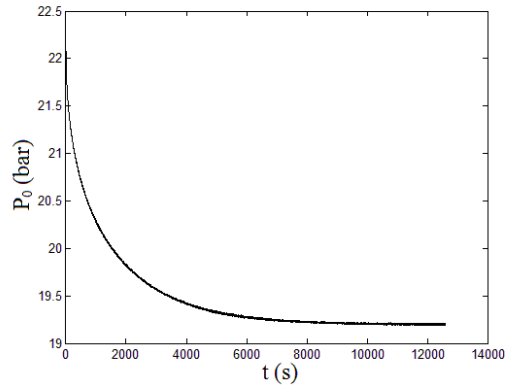


Figure 4. Pressure decay curves for the different  $(k_1, b)$  pairs reported in table 1

This figure, where all pressure signals are superimposed, highlights a key point related to the pulse decay experiment on crushed core plugs: the difficulty to discriminate the independent role of  $k_1$  and  $b$  on a given pressure decay. Indeed, the direct simulations show that the same signal can be obtained from tests performed with different combinations of the two parameters  $k_1$  and  $b$  that can be varied over an order of magnitude (and even more). The physical explanation of this behavior is as follows. Because the pressure decay remains small, the Klinkenberg term  $b/P$  experiences small variations so that  $k_1(1 + b/P)$  remains quasi constant during the test making impossible the identification of the separate role of  $k_1$  and  $b$  on  $P_0(t)$ . In other words, this indicates that  $k_1$  and  $b$  appear as correlated parameters for the signal  $P_0(t)$ , a feature that is more pronounced when  $k_1$  (and  $\phi$ ) are small, as for instance in the range of interest for tight or gas shale reservoirs. A clear



illustration can be made from the sensitivity of  $P_0(t)$  to each of the three parameters,  $k_1$ ,  $b$  and  $\phi$ .

The reduced sensitivity  $(S_r)_i$  of the measured pressure  $P_0$  to the parameter  $\theta_i$  is defined by:

$$(S_r)_i = \theta_i \frac{\partial P_0}{\partial \theta_i} \tag{17}$$

It basically expresses how the evolution of  $P_0$  is modified upon a slight modification of the parameter  $\theta_i$ , all other parameters remaining the same. It should be noted that the identification of  $\theta_i$  from  $P_0(t)$  is possible only if  $(S_r)_i$  is larger than the sensitivity of the pressure sensor used to measure  $P_0(t)$ . An optimal estimation of  $\theta_i$  also requires that the experiment is designed to maximize  $(S_r)_i$  and minimize the  $\theta_i$  to  $\theta_j$  correlation.

Two different parameters  $\theta_i$  and  $\theta_j$  are correlated when their respective sensitivities  $(S_r)_i$  and  $(S_r)_j$  are proportional. In figure 5a, we have represented the sensitivity curves of  $P_0(t)$  to  $k_1$ ,  $b$  and  $\phi$  using  $k_1=10^{-21} \text{ m}^2$ ,  $b=68.6 \cdot 10^5 \text{ Pa}$ ,  $\phi = 1 \%$ ,  $R_0=10^{-2} \text{ m}$ ,  $V_0=20 \cdot 10^{-6} \text{ m}^3$ ,  $V_1=75.4 \cdot 10^{-6} \text{ m}^3$ ,  $DV=26.5 \cdot 10^{-6} \text{ m}^3$ ,  $P_{1i}=10^5 \text{ Pa}$ ,  $\mu=1.8 \cdot 10^{-5} \text{ Pa}\cdot\text{s}$ ,  $t_f=1400 \text{ s}$ ,  $NP=14000$  and  $m=200$ .

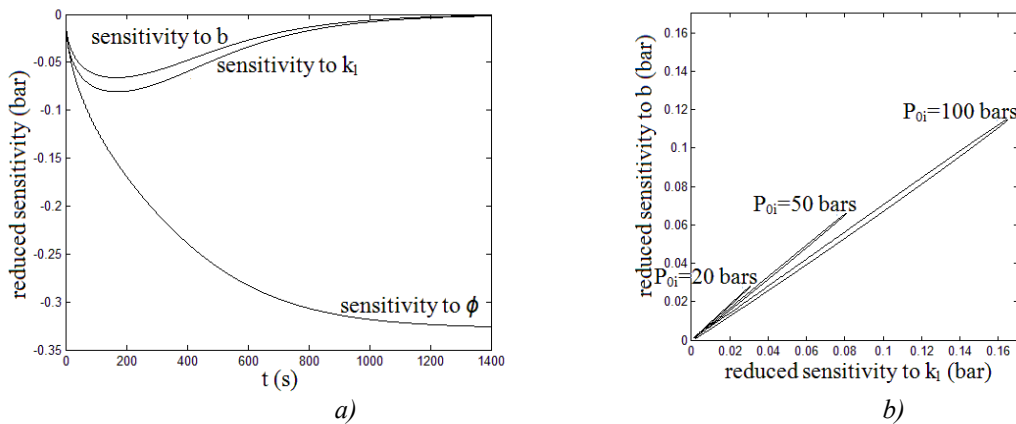


Figure 5. a) Sensitivity curves to  $k_1$ ,  $b$  and  $\phi$  for  $P_{0i}=50 \cdot 10^5 \text{ Pa}$ . b)  $k_1$ - $b$  correlation curves (in absolute value) for different pressure pulses  $P_{0i}$

Clearly, the sensitivity of  $P_0(t)$  to  $\phi$  greatly exceeds those to  $k_1$  and  $b$ , the latter being the lowest one. The large sensitivity to  $\phi$  is indeed expected since the pulse decay test in that case is a pycnometry-type experiment, a result that contrasts with the classical pulse decay test performed on an entire plug. All the three sensitivities remain large compared to the precision of a standard pressure sensor.

Figure 5b points out the correlation of  $k_1$  and  $b$  for moderate pressure pulses  $P_{0i}$  (~50 bars and less) through the quite perfect straight lines of the graph representing the sensitivity to  $b$  versus that to  $k_1$ . Using larger pressure pulses, near 100 bars and more, slightly weakens

the correlation in accordance with the fact that the apparent local permeability  $k_1 \left(1 + \frac{b}{P}\right)$  experiences larger variations over the pressure decay period. However, with such an experimental design, the correlation remains so significant that the simultaneous



identification of the three parameters  $k_l$ ,  $b$  and  $\phi$  is seriously compromised as further analyzed in the next section.

### Inverse Procedure

The pressure decay signal inversion is operated using a Levenberg-Marquardt numerical algorithm as in [9]. This method which is commonly used to treat least square curve fitting problems returns the vector of parameters  $\Theta$  ensuring the best correspondence between a set of empirical data  $(t_i, p_i)$  and the estimated values  $P(t_i, \Theta)$  derived from the solution to the direct problem. Optimal estimated parameters are found by minimizing the quadratic residues:

$$S(\Theta) = \sum_{i=1}^{NP} [p_i - P(t_i, \Theta)]^2 \quad (18)$$

The inverse procedure was run for two configurations of permeability and porosity. In both cases, the pressure decay signal was generated using the direct simulation detailed above while superimposing a Gaussian noise which amplitude was fixed according to the pressure decay magnitude (see tables 2 and 3) to guarantee the convergence of the algorithm. Inversion was started giving two different initial sets  $(k_{lm}, b_m, \phi_m)_j$ . The  $(b_m)_j$  were chosen according to the correlation proposed by Jones [10]:

$$(b_m)_j = 0.189 \left( (k_{lm})_j \right)^{-0.36} \quad (19)$$

whereas the  $(\phi_m)_j$  were taken equal to the nominal value  $\phi$ . Note that since the final equilibrium pressure  $P_f$  satisfies:

$$P_f = \frac{P_{0i} V_0 + P_{1i} (DV + \phi V_1)}{V_0 + DV + \phi V_1} \quad (20)$$

$\phi$  can be effectively pre-estimated with accuracy if the various pressures and volumes needed for the calculation are measured with care and the experiment is long enough to reach final equilibrium. Direct simulations and inversions were carried out with the following parameters:  $R_0=10^{-2}$  m,  $V_0=20 \cdot 10^{-6}$  m<sup>3</sup>,  $V_1=75.4 \cdot 10^{-6}$  m<sup>3</sup>,  $DV=26.5 \cdot 10^{-6}$  m<sup>3</sup>,  $P_{0i}=50 \cdot 10^5$  Pa,  $P_{1i}=10^5$  Pa,  $\mu=1.8 \cdot 10^{-5}$  Pa.s and  $m=200$ . The results of the inversion are gathered in tables 2 and 3.

Table 2. Estimates of  $k_l$ ,  $b$  and  $\phi$  in case 1 ( $t_f=50$  s,  $NP=500$ ). Pressure decay amplitude: 2.57 bars. -10 mbars < noise amplitude < 10 mbars

	Real value	Starting value	Estimated value	Error (%)
$k_l$ (m <sup>2</sup> )	$10^{-18}$	$(k_{lm})_1=2. \cdot 10^{-18}$	$9.25 \cdot 10^{-19}$	7.5
		$(k_{lm})_2=6. \cdot 10^{-19}$	$8.45 \cdot 10^{-19}$	15.5
$b$ (Pa)	$5.71 \cdot 10^5$	$(b_m)_1=4.45 \cdot 10^5$	$7.28 \cdot 10^5$	27.5
		$(b_m)_2=6.86 \cdot 10^5$	$9.29 \cdot 10^5$	62.0
$\phi$	0.1	$(\phi_m)_1=0.1$	0.1	0
		$(\phi_m)_2=0.1$	0.1	0

Table 3. Estimates of  $k_1$ ,  $b$  and  $\phi$  in case 2 ( $t_f=1400$  s,  $NP=14000$ ). Pressure decay amplitude: 330 mbars - 1 mbar < noise amplitude < 1 mbar

	Real value	Starting value	Estimated value	Error (%)
$k_1$ (m <sup>2</sup> )	$10^{-21}$	$(k_{1,m})_1=7. \cdot 10^{-21}$	$1.61 \cdot 10^{-21}$	61.0
		$(k_{1,m})_2=3. \cdot 10^{-22}$	$4.36 \cdot 10^{-22}$	56.4
$b$ (Pa)	$68.6 \cdot 10^5$	$(b_m)_1=34.1 \cdot 10^5$	$36.8 \cdot 10^5$	46.4
		$(b_m)_2=10.59 \cdot 10^6$	$11.74 \cdot 10^6$	71.1
$\phi$	0.01	$(\phi_m)_1=0.01$	0.01	0
		$(\phi_m)_2=0.01$	0.01	0

As expected, the strong correlation between  $k_1$  and  $b$  explained above justifies the fact that the estimated values are dependent upon the starting data. Despite the weak discrepancies between the starting and real vectors of parameters and despite also the relatively small amplitude of the superimposed noise, errors on  $k_1$  and  $b$  are quite large. This analysis clearly shows that: *i*) convergence can only be achieved if initial values of  $k_1$  and  $b$  are extremely close to the actual values; *ii*) when convergence is achieved, uncertainty on the estimated values of the parameters can be very large, and increases when  $k_1$  decreases.

Although larger pressure pulses could be used to induce larger pressure decays reducing slightly the correlation between  $k_1$  and  $b$ , this may cause experimental artifacts due to pressure fluctuations and thermal effects associated to abrupt pressure drop at valve opening as well as mechanical effects on the porous particles. Since the small variation of the apparent permeability causing correlation between  $k_1$  and  $b$  is due to a large volume  $V_0+DV$  compared to the pore volume  $\phi V_1$ , an alternative is to considerably reduce  $V_0$  and/or  $DV$ . In the remaining part of this work,  $V_0$  is considered to be 0 (more precisely, in the above numerical model,  $DV$  is set to zero while  $V_0$  is taken as the actual value of  $DV$ ) so that  $V_S$  is directly connected to the gas supply. The actual experimental situation would be that of Fig. 1 for which the valve between  $V_0$  and  $V_S$  is opened in order to supply gas and generate the pulse and then closed so that the available gas volume is  $DV$  only during the whole test. This configuration is now considered and to reduce even more  $V_0$  (i.e.  $DV$ ), a sample made of a single spherical particle having the volume of the standard core plug is chosen. Under these circumstances, reliable estimates of  $k_1$ ,  $b$  (and  $\phi$ ) are obtained since inversion yields identical results whatever the starting values of the parameters, provided that they lead to convergence. In this situation, the objective is now to investigate the error on the parameters  $k_1$ ,  $b$  and  $\phi$  estimated by inversion due to bias on the volume of the chamber  $V_0$  and on the sample volume  $V_1$  that may always occur due to measurement errors on these two parameters.

Table 4. Errors on the estimates of  $k_1$ ,  $b$  and  $\phi$ , due to a bias of 2 % on  $V_0$  and 6 % on  $V_1$

	Estimated values			Errors		
	$k_1$ (m <sup>2</sup> )	$b$ (Pa)	$\phi$	$\Delta k_1/k_1$ (%)	$\Delta b/b$ (%)	$\Delta \phi / \phi$ (%)
$V_0+\Delta V_0$	$1.02 \cdot 10^{-17}$	$2.49 \cdot 10^5$	0.102	2.0	0	2.0
$V_0-\Delta V_0$	$9.80 \cdot 10^{-18}$	$2.49 \cdot 10^5$	0.098	2.0	0	2.0

$V_1+\Delta V_1$	$5.15 \cdot 10^{-18}$	$2.49 \cdot 10^5$	0.050	48.5	0	50.0
$V_1-\Delta V_1$	$1.48 \cdot 10^{-17}$	$2.49 \cdot 10^5$	0.154	48.0	0	54.0

To do so, pressure decay signals were generated with the nominal values of  $V_0$  and  $V_1$  while respective bias of  $\pm 2\%$  on  $V_0$  and  $\pm 6\%$  on  $V_1$  were introduced to carry out the inversion. It should be noted that a bias on  $V_1$  is unavoidably reflected in  $V_0$  ( $V_0=DV=V_S-V_1$ ). Tests were performed with  $k_1=10^{-17} \text{ m}^2$ ,  $b=2.49 \cdot 10^5 \text{ Pa}$ ,  $\phi=10\%$ ,  $R_0=2.6 \cdot 10^{-2} \text{ m}$ ,  $V_0=9.8 \cdot 10^{-6} \text{ m}^3$ ,  $V_1=75.4 \cdot 10^{-6} \text{ m}^3$ ,  $DV=0 \text{ m}^3$ ,  $P_{0i}=50 \cdot 10^5 \text{ Pa}$ ,  $P_{1i}=10^5 \text{ Pa}$ ,  $t_f=30 \text{ s}$ ,  $NP=300$ ,  $\mu=1.8 \cdot 10^{-5} \text{ Pa}\cdot\text{s}$  and  $m=200$ .

Results of the inverse procedure are reported in table 4. They clearly show that the estimation of the Klinkenberg coefficient is insensitive to bias on both  $V_0$  and  $V_1$ . In addition, a bias on  $V_0$  seems to be directly reflected in  $k_1$  and  $\phi$  which means that the expected error due to this bias is not very significant provided the volume chamber is carefully characterized. However, the results show that the bias on  $V_1$  has a very strong impact on both  $k_1$  and  $\phi$  requiring that the volume of the crushed sample must be very carefully measured if one is willing to extract reliable information on both  $k_1$  and  $\phi$  from the pulse decay signal.

## CONCLUSION

A direct model and the related inverse procedure were proposed to characterize in depth the physical properties of a crushed porous medium using a pulse decay test. From this analysis, it appears first that the available information in the pressure decay signal is intimately related to the particle size of the crushed sample. If small particle radii are used, the pulse relaxation time, which is even reduced for increasing permeabilities, may be so small that no interpretation of the pressure decay signal is possible. This suggests that a pre-estimation (for instance on an entire core-plug) of the order of magnitude of both  $k_1$  and  $\phi$  would advantageously help defining the appropriate particle mean radius for a further pulse decay experiment on the crushed sample. A sensitivity analysis performed on the pressure decay indicates that, for a standard experimental design, the identification of both  $k_1$  and  $b$  is seriously compromised due to the fact that these two parameters are strongly correlated. The physical origin of this lies in the restricted variation of the apparent gas permeability during the test. Without any pre-estimation (for instance on an entire core-plug) of the order of magnitude of both  $k_1$  and  $b$ , their estimation on crushed rock might be off by an order of magnitude. Conversely, and as expected, if volumes of both the chambers  $V_0$  (and  $DV$ ) and porous sample ( $V_1$ ) are well characterized, a precise determination of the porosity can be performed as in a classical pycnometry-type experiment. Finally, a quick analysis of the impact of the bias on both  $V_0$  and  $V_1$  shows that, when the inversion can be performed, the resulting estimated values of  $b$  are unaffected by these bias. The bias on  $V_0$  may not be very significant on both  $k_1$  and  $\phi$  since it seems to be directly reflected as an error on the estimated values of these coefficients. On the contrary, a bias on  $V_1$  induces very significant errors on both  $k_1$  and  $\phi$  suggesting that the volume of the crushed porous sample must be precisely measured for a reliable identification of these two parameters from the pulse decay signal.

## NOMENCLATURE

b	Klinkenberg coefficient (Pa)	$S_T$	particles total exchange area ( $m^2$ )
DV	dead volume ( $m^3$ )	$t/t_i$	time/ $i^{\text{th}}$ date of measurement (s)
$k_l$	intrinsic permeability ( $m^2$ )	$t_f$	duration of the experiment (s)
m	number of space nodes (-)	$V_s$	sample cell volume ( $m^3$ )
NP	number of measurement point (-)s	$V_0$	reference cell volume ( $m^3$ )
$P/p_i$	gas pressure/ $i^{\text{th}}$ experimental datum (Pa)	$V_1$	crushed sample volume ( $m^3$ )
$P_{0i}$	initial pressure pulse (Pa)	$\beta_f$	ideal gas compressibility ( $Pa^{-1}$ )
$P_0(t)$	pressure at $r=R_0$ and t (Pa)	$\Delta r$	node spacing (m)
$P_{li}$	initial steady-state pressure (Pa)	$\Delta t$	time step (s)
$P_m$	mean value of $P_0$ over $t_f$ (Pa)	$\Delta X/X$	relative bias on X (-)
r	radial coordinate (m)	$\phi$	porosity (-)
$R_0$	particle radius (m)	$\Theta/\theta_i$	vector of parameters/ $i^{\text{th}}$ parameter
S	sum of the squares of the residues ( $Pa^2$ )	$\mu$	dynamic viscosity (Pa.s)
$S_r$	reduced sensitivity (Pa)		

## REFERENCES

1. Brace, W. F., Walsh, J. B., Frangos, W. T., "Permeability of Granite Under High Pressure", *Journal of Geophysical Research*, (1968) **73**, 6, 2225-2236.
2. Luffel, D. L., Hopkins, C. W., Shettler, P. D., "Matrix Permeability Measurement of Gas Productive Shales", 68<sup>th</sup> Annual Technical Conference and Exhibition of the Society of Petroleum Engineers, Houston, Texas, 3 – 6 October 1993. SPE 26633.
3. Egermann, P., Lenormand, R., Longeron, D., Zarcone, C., "A Fast and Direct Method of Permeability Measurement on Drill Cuttings", *Petrophysics*, (2003) **44**, 4, 243-252.
4. Lenormand, R., Bauget, F., Ringot, G., "Permeability Measurement on Small Rock Samples", International Symposium of the Society of Core Analysts, Halifax, Nova Scotia, Canada, 4 – 7 October 2010.
5. Wang, Y., Knabe, R. J., "Permeability Characterization on Tight Gas Samples Using Pore Pressure Oscillation Method", International Symposium of the Society of Core Analysts, Halifax, Nova Scotia, Canada, 4 – 7 October 2010.
6. Jannot, Y., Lasseux, D., Vizé, G., Hamon, G., "A Detailed Analysis of Permeability and Klinkenberg Coefficient Estimation from Unsteady-State Pulse-Decay or Draw-Down Experiments", International Symposium of the Society of Core Analysts, Calgary, Canada, 10 – 12 September 2007.
7. Hsieh, P. A., Tracy, J. V., Neuzil, C. E., Bredehoeft, J. D., and Silliman, S. E., "A Transient Laboratory Method for Determining the Hydraulic Properties of Tight Rocks – 1. Theory", *International Journal of Rock Mechanics and Mining Sciences & Geomechanics Abstracts*, (1980) **18**, 3, 245-252.
8. Wu, Y. – S., Pruess, K., Persoff, P., "Gas Flow in Porous Media with Klinkenberg Effects", *Transport in Porous Media*, (1998) **32**, 1, 117-137.
9. Jannot, Y., Lasseux, D., Delottier, L. and Hamon, G., "A Simultaneous Determination of Permeability and Klinkenberg Coefficient from an Unsteady-State Pulse-Decay Experiment", International Symposium of the Society of Core Analysts, Abu Dhabi, October 29 – November 2 2008.
10. Jones S.C., "A Rapid and Accurate Unsteady-State Klinkenberg Permeameter", *SPE Journal*, (1972) **12**, 5, 383-397. SPE 3535.